

# Alkane Hydroxylation by Peroxy Acids: A Comparison with the Cytochrome P450 Hydroxylation<sup>†</sup>

André R. Groenhof, Andreas W. Ehlers, and Koop Lammertsma\*

Vrije Universiteit, FEW, Department of Chemistry, De Boelelaan 1083, 1081 HV Amsterdam, The Netherlands

Received: February 27, 2008; Revised Manuscript Received: September 25, 2008

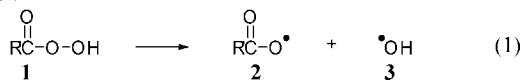
Alkane hydroxylation by peroxy acids proceeds by a synchronous nonconcerted peroxy oxygen insertion into the C–H bond according to density functional theory. A comparable reaction sequence, initiated by homolytic peroxy bond cleavage, can be formulated for the alkane hydroxylation by the cytochrome P450 hydroperoxo-heme Compound 0. This hydroxylation reaction proceeds by a two-step process because the formed reactive intermediate, Compound II, is significantly stabilized.

## Introduction

Controlled oxidation reactions under mild conditions, like those with peroxyacids, are one of the most important tools developed by synthetic chemists in the past centuries.<sup>1–8</sup> Nature instead makes use of the catalytic function of the iron–heme prosthetic in oxidoreductase enzymes, e.g., catalases, peroxidases, and heme–thiolate proteins. Are there similarities between the two types of oxidations? To address this question, we focus on the mechanism of oxidation of hydrocarbons by peroxyacids and make comparisons with that by the heme-thiolate protein cytochromes P450, which has been studied intensely for many years. The presence of minor amounts of radical derived side products during alkane hydroxylation with peroxy acids (CO<sub>2</sub>, CHF<sub>3</sub> when R' = CF<sub>3</sub>; chlorobenzene when R' = C<sub>6</sub>H<sub>4</sub>Cl) suggests the involvement of radical intermediates. On the other hand, the high stereo- and regioselectivity is indicative of a concerted oxygen insertion.<sup>9</sup>

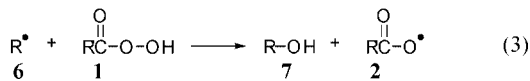
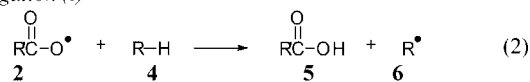
Homolytic O–O bond cleavage presumably initiates the free radical peroxy acid hydroxylation (eq 1).<sup>10</sup> The propagation steps involve hydrogen abstraction from an unactivated hydrocarbon followed by decomposition of a second peracid molecule by the alkyl radical (eqs 2 and 3). Decarboxylation of the acyloxy radical gives a competing hydrogen abstracting species (eqs 4 and 5). However, these free radical processes are not consistent with the experimentally observed stereoselectivity.<sup>8</sup> Therefore, another propagation mechanism has been proposed (eqs 6 and 7) in which hydrogen abstraction from the peroxy acid (**1**) by the acyloxy radical (**2**) takes place to generate a peroxy radical (**1** → **2**) that selectively abstracts a hydrogen atom from the unactivated hydrocarbon.<sup>12</sup> The high degree of configurational retention in the oxidation of epimeric cycloalkanes has been attributed to a fast hydrogen abstraction and oxygen rebound cage reaction (eq 7).<sup>8</sup>

### Initiation

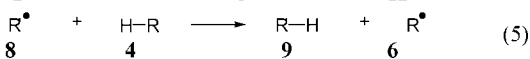
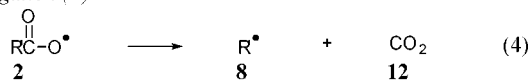


In the concerted peroxy acid hydroxylation the alkane hydrogen transfer to the peroxy oxygen atom and O–O bond

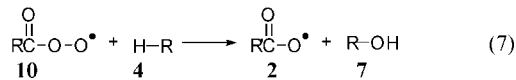
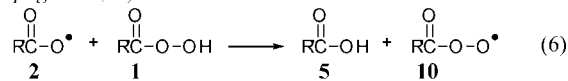
### Propagation (I)



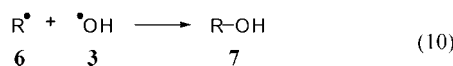
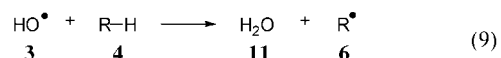
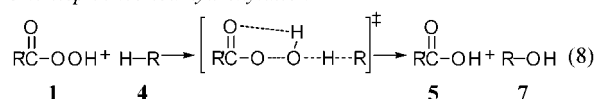
### Propagation (II)



### Propagation (III)



### One step concerted hydroxylation

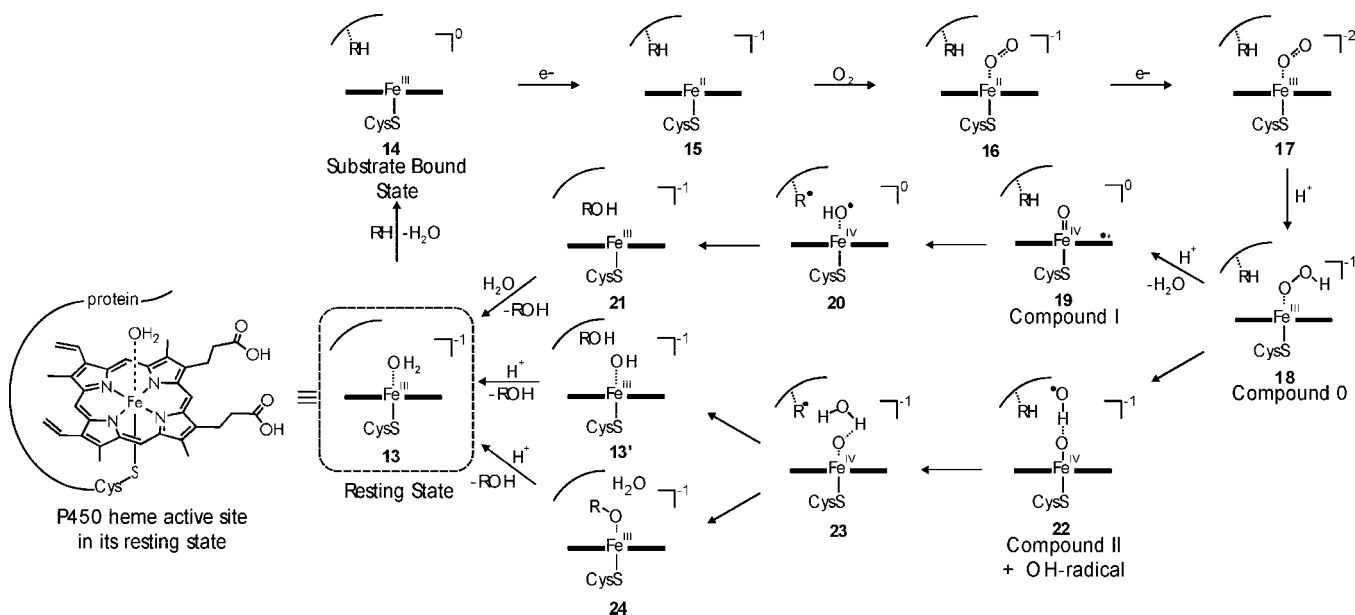


cleavage occur concurrently.<sup>12–15</sup> Two routes are feasible. Either the alkyl–water–acyloxy triad transition state gives the protonated alcohol product (eq 8), followed by proton transfer to the R'-formate anion, or the alkyl group is separated to form the alkyl and R'-formate radicals that initiate the reactions that are associated with the observed byproducts.<sup>11,12</sup>

There are apparent similarities with the two-electron oxidation by Cytochromes P450 where one of the oxygen atoms derived from dioxygen inserts, for example, into the C–H bond of substrate RH.<sup>16</sup> The generally accepted mechanism consists of 8 steps shown in Scheme 1. These include substrate binding into the active site; first reduction; binding of molecular oxygen to the heme iron; second reduction; protonation to afford the

<sup>†</sup> Part of the “Sason S. Shaik Festschrift”.

\* Corresponding author. E-mail: K.Lammertsma@few.vu.nl.

SCHEME 1: Cytochrome P450 Catalytic Reaction Cycle<sup>a</sup>

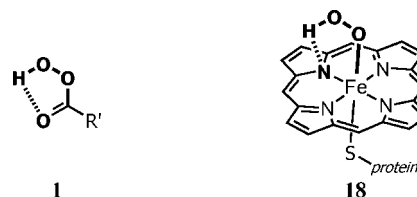
hydroperoxy iron heme species (**13**  $\rightarrow$  **18**) (Compound 0); heterolytic peroxy O–O bond cleavage to generate a water molecule and the iron(IV) oxo porphyrin radical  $\pi$ -cation **19** (Compound I) that, subsequently, abstracts a hydrogen atom from the substrate (**19**  $\rightarrow$  **20**); and finally, the substrate radical rebounding to the radical oxygen atom to yield the alcohol product (**20**  $\rightarrow$  **21**).<sup>17,18</sup> The first 5 steps of this catalytic cycle, up to the formation of the hydroperoxy complex **18**, are generally agreed upon,<sup>19–22</sup> and there is a growing consensus for the following ones.<sup>23–25</sup> The discussion, relevant to the present study, concerns the fate of the peroxy O–O bond. Besides, it is generally accepted *heterolytic* cleavage, a *homolytic* cleavage has been proposed on the basis of experimental support.<sup>26</sup> Homolytic cleavage would generate an iron(IV) oxo porphyrin complex (Compound II) and a hydroxyl radical (**18**  $\rightarrow$  **22**) that might abstract a hydrogen atom from the substrate to give a carbon radical and a water molecule (**23**).<sup>27</sup> Subsequent hydroxylation has been postulated to involve a concerted H-transfer from the water molecule to the iron(IV) oxo porphyrin complex with concomitant rebound of the carbon radical to the incipient hydroxyl radical (**23**  $\rightarrow$  **13'**).<sup>27</sup> The rebound might also take place between the carbon radical and the oxygen atom of the iron(IV) oxo porphyrin complex (**23**  $\rightarrow$  **24**) to form an alkoxy iron heme complex as a key intermediate.<sup>27</sup>

The oxidation chemistry of the cytochromes P450 may show analogies to that of the peroxy acids not only with respect to the stereo- and regioselective hydroxylation of unactivated hydrocarbons<sup>1–8</sup> but also whether the oxygen insertion occurs in a stepwise radical or a concerted manner.<sup>6,7</sup> For example, stepwise (free) radical and concerted oxygen insertion have been assumed to take place concurrently. These apparent structural similarities of the peroxy acids with Compound 0 of the cytochromes P450 (Scheme 2) were an additional encouragement to investigate the noncatalytic and nonenzymatic peroxy acid hydroxylation, using density functional theory.

## Computational Details

Calculations were performed with the Amsterdam Density Functional (ADF) program.<sup>28</sup> The atomic orbitals on all atoms were described by an uncontracted triple- $\zeta$  valence plus

## SCHEME 2: Cytochromes P450 Hydroperoxy Iron Porphyrin Intermediate Compound 0 (Right) and the Corresponding Peroxy Acid (Left)



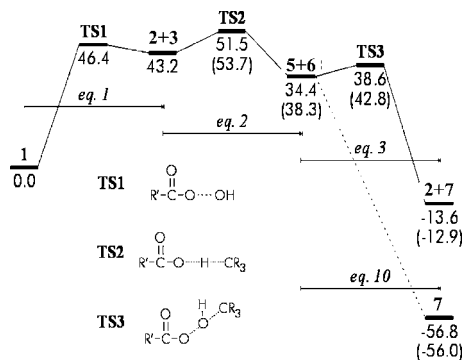
polarization STO basis set (TZP). The inner cores of carbon, nitrogen, and oxygen ( $1s^2$ ) and those of sulfur and iron ( $1s^22s^22p^6$ ) were kept frozen. The exchange-correlation potential is based on the newly developed GGA exchange functional OPTX<sup>29</sup> in combination with the nonempirical PBE<sup>30</sup> (OPBE). Solvent effects ( $\text{CH}_2\text{Cl}_2$ ,  $\epsilon = 8.9$ ) are included by using a polarizable continuum model (COSMO).<sup>31</sup> The vibrational eigenvectors associated with the imaginary frequency of all transition states were analyzed to confirm the connectivity of transition states with the reactants and the products.

## Results and Discussion

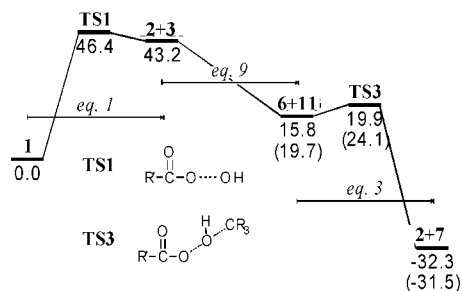
The oxidation of propane and butane by the common oxidant *m*-chloroperbenzoic acid (*m*CPBA) was investigated at OPBE/TZP. Free-radical mechanisms initiated by homolytic O–O bond cleavage followed by several pathways for propagation (eqs 1–7) are described first. Next, a non-free-radical route is described. This is followed by a comparison of the two peroxy acid oxidation mechanisms. Finally, a comparison is made with the analogous chemistry of cytochromes P450 alkane hydroxylation.

**Free Radical Mechanisms.** Homolytic O–O bond cleavage initiates the free radical peroxy acid hydroxylation mechanism (eq 1). This first step, generating the *m*-chlorobenzoate (**2**) and the hydroxyl radicals, is  $43.2 \text{ kcal mol}^{-1}$  endothermic<sup>32</sup> and has an activation energy of  $46.4 \text{ kcal mol}^{-1}$  (TS1). We consider four different propagation reactions: (a) direct hydrogen abstraction from the alkane by the *m*-chlorobenzoate radical (eq 2), (b) direct hydrogen abstraction from the alkane by the hydroxyl

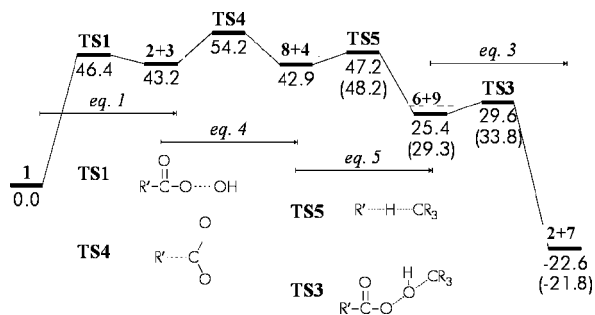
**SCHEME 3: Energy Profiles for the Stepwise Hydroxylation of Butane and Propane (Values in Parentheses) Initiated by Homolytic O–O Bond Cleavage in *m*CPBA Followed by Hydrogen Abstraction by the *m*-Chlorobenzoate Radical**



**SCHEME 4: Energy Profiles for the Stepwise Hydroxylation of Butane and Propane (Values in Parentheses) Initiated by Homolytic O–O Bond Cleavage in *m*CPBA Followed by Hydrogen Abstraction by the Generated Hydroxyl Radical**



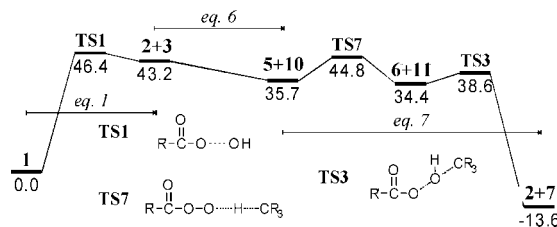
**SCHEME 5: Energy Profiles for the Stepwise Hydroxylation of Butane and Propane (Values in Parentheses) Initiated by Homolytic O–O Bond Cleavage in *m*CPBA Followed by CO<sub>2</sub> Dissociation**



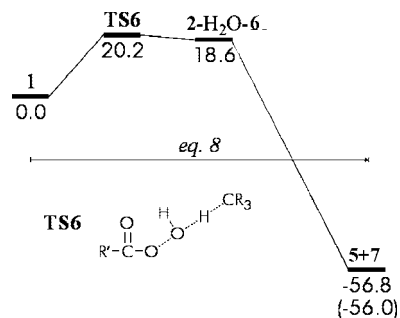
radical (eq 9), (c) initial dissociation into CO<sub>2</sub> and the *m*-chlorophenyl radical (eq 4), and (d) hydrogen abstraction from a second *m*CPBA molecule to generate the active *m*-chlorobenzoperoxoate radical (eq 6). The hydroxylations invoking each of these propagation steps will be described for butane. The energy profiles are given in Schemes 3–6 and transition structures are shown in Figure 1.

**Path a (Scheme 3).** Hydrogen abstraction from butane by *m*-chlorobenzoate radical **2** (eq 2) is exothermic by 8.8 kcal mol<sup>-1</sup> and has a barrier (TS2) of 8.3 kcal mol<sup>-1</sup>. The next step involves the hydroxylation of carbon radical **6** by a second *m*-CPBA molecule (eq 3). Homolytic O–O bond cleavage in *m*-CPBA in concord with C–O bond formation has a barrier of only 4.2 kcal mol<sup>-1</sup> (TS3) and generates the *m*-chlorobenzoate radical and the butanol product exothermically by –48.0

**SCHEME 6: Energy Profiles for the Stepwise Hydroxylation of Butane and Propane (Values in Parentheses) Initiated by Homolytic O–O Bond Cleavage in *m*CPBA Followed by the Formation of the Active *m*-Chlorobenzoperoxoate Radical 10**

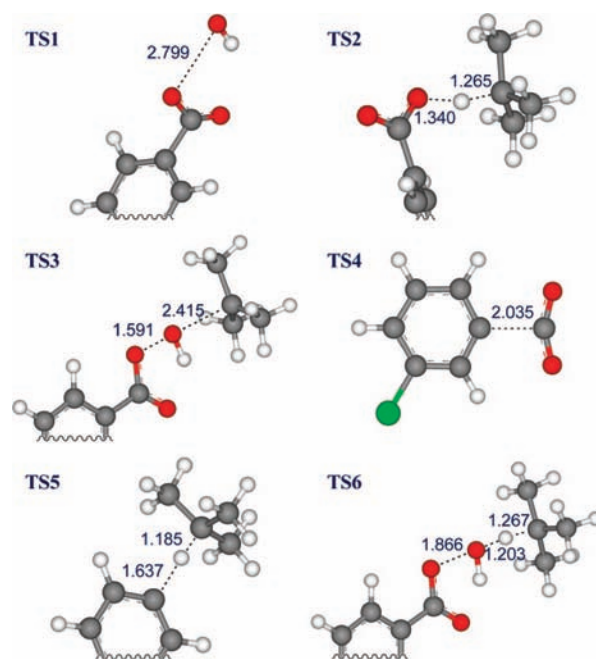


**SCHEME 7: Energy Profiles for the Non-Free-Radical Hydroxylation of Butane and Propane (Values in Parentheses) by MCPBA**

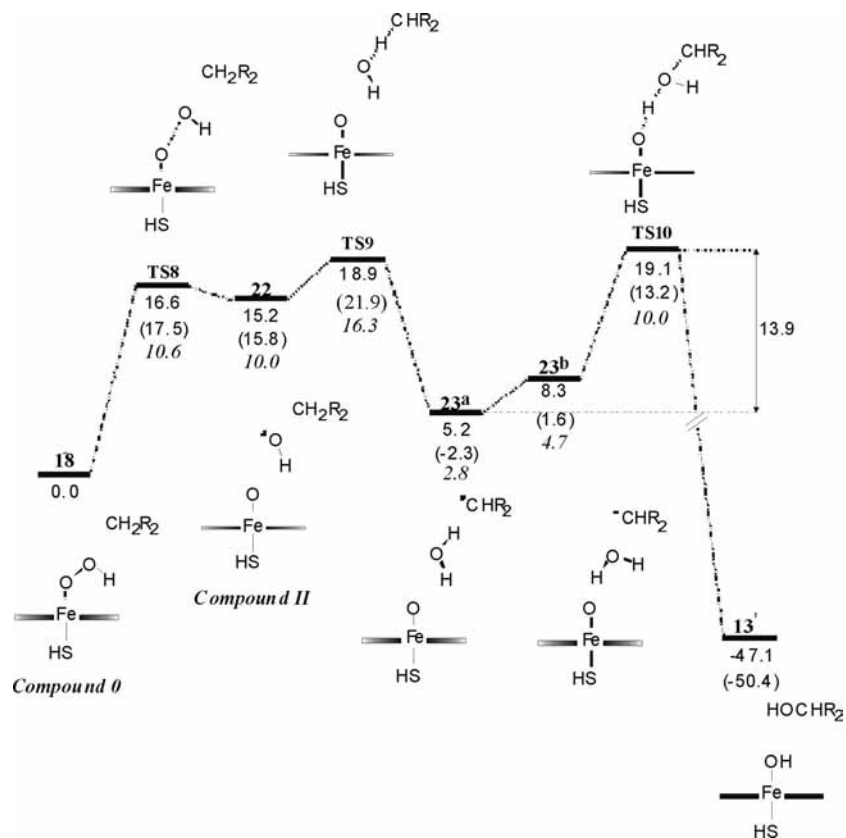


kcal mol<sup>-1</sup> (eq 3). The barrier-free C–O bond formation between the hydroxyl and butyl radicals is the preferred and highly exothermic reaction to give the alcohol (eq 10; Δ*E* = –91.2 kcal mol<sup>-1</sup>). The energy released by C–O bond formation is about twice that needed for cleaving the O–O bond in **1** (91.2 vs 43.2 kcal mol<sup>-1</sup>) due to better (resonance) stabilization of acid radical **2** compared to carbon radical **6**. This energy gain provides ample driving force for the propagation steps.

**Path b (Scheme 4).** Hydrogen abstraction by the free hydroxyl radical (eq 9) generates the carbon radical and a water molecule



**Figure 1.** Transition structures of Schemes 4–8 with selected bond distances (Å).

**SCHEME 8: Energy Profile for the Compound 0 Hydroxylation of Methane (R = H) with Those for Propane (R = CH<sub>3</sub>) in Parentheses<sup>a</sup>**


<sup>a</sup> Values in italic include solvation.

in a barrier-free 27.4 kcal mol<sup>-1</sup> exothermic reaction.<sup>33</sup> Subsequent hydroxylation of the carbon radical by a second *m*-CPBA molecule via **TS3** yields alcohol product **7**.

**Path c (Scheme 5).** Dissociation of CO<sub>2</sub> from *m*-chlorobenzoate radical **2** is thermoneutral (eq 4;  $\Delta E = -0.2$  kcal mol<sup>-1</sup>) with a barrier of 11.0 kcal mol<sup>-1</sup> (**TS4**). Subsequent H-abstraction from butane by *m*-chlorophenyl radical **8** has a barrier of only 4.3 kcal mol<sup>-1</sup> (**TS5**) generating chlorobenzene and the butyl radical exothermically by 17.5 kcal mol<sup>-1</sup>. Concerted homolytic O–O bond cleavage in a second *m*-CPBA molecule and C–O bond formation results in the 48.0 kcal mol<sup>-1</sup> exothermic formation of butanol ( $\Delta E^\ddagger$  4.2 kcal mol<sup>-1</sup> (**TS3**)).

**Path d (Scheme 6).** Finally, formation of *m*-chlorobenzoperoxoate radical **10** by hydrogen transfer from *m*-CPBA to *m*-chlorobenzoate radical **2** is exothermic (by 7.5 kcal mol<sup>-1</sup> and barrier-free; eq 6). Subsequent butane hydroxylation involves H-abstraction by radical **10** ( $\Delta E^\ddagger$  9.1 kcal mol<sup>-1</sup>) to give the isobutane radical and the *m*-CPBA molecule that react via the described transition state **TS3**.

Utilizing propane instead of butane gives almost the same energy profile with only slightly less stable transition structures and intermediates (Schemes 3–6, values in parentheses), which is a consequence of the reduced stabilization of a secondary radical with respect to a tertiary one.

**Non-Free-Radical Mechanism.** Is there an alternative to the multistep mechanism, bypassing the initial homolytic O–O bond cleavage of *m*-CPBA that leads to the series of steps, culminating in the formation of the hydroxylated alkane, as experimental studies have suggested?<sup>25–27</sup> An extensive search of the potential energy surface indeed revealed a complex concerted process in which various features of the reaction occur simultaneously

during a single step. This can be formulated as follows: hydrogen atom abstraction from butane occurs concurrently with homolytic O–O cleavage to generate an incipient carbon radical that concomitantly binds to the oxygen atom of the developing water molecule. This process requires 20.2 kcal mol<sup>-1</sup> (Scheme 7). The transition structure is shown as **TS6** in Figure 1. In the transition state the bonds that are broken and formed are almost in a straight line ( $\theta_{\text{CHO}} = 173.016^\circ$ ;  $\theta_{\text{HOO}} = 179.140^\circ$ ). The O–O bond distance is 1.866 Å and those between the radical carbon center and the H-atom of the developing water molecule and between this hydrogen atom and the oxygen of the hydroxyl group are 1.267 and 1.203 Å, respectively. The immediate product of the 18.6 kcal mol<sup>-1</sup> endothermic concerted process is a triad of a butyl radical, a water molecule, and a *m*-chlorobenzoate radical. This triad is a minimum on the potential energy surface, which is, however very flat. Rotation of the water molecule in this triad for which no transition could be determined and subsequent C–O bond formation together with a hydrogen shift from the intervening water molecule to the *m*-chlorobenzoate moiety results in the barrier-free exothermic (–75.4 kcal mol<sup>-1</sup>) formation of butanol and *m*-chlorobenzoic acid.

**Comparison of the Free and Non-Free-Radical Mechanisms.** Generation free radicals by homolysis of the peroxy O–O bond of *m*CPBA is quite an endothermic process (43.2 kcal mol<sup>-1</sup>) with a correspondingly high reaction barrier (46.4 kcal mol<sup>-1</sup>). The concerted mechanism on the other hand, with the concurrent H-abstraction from butane and O–O bond cleavage, has a much more modest activation energy (20.2 kcal mol<sup>-1</sup>). In either case, formation of the products butanol and *m*-chlorobenzoic acid is highly favorable (–56.8 kcal mol<sup>-1</sup>). Could solvents influence the energy profiles? With di-

**TABLE 1: Activation (EA) and Reaction ( $\Delta E$ ) Energies (in kcal mol<sup>-1</sup>) for the Unactivated and Butane Activated Homolytic O–O Bond Cleavage in Vacuo and in Dichloromethane**

	unactivated		butane activated	
	EA	$\Delta E$	EA	$\Delta E$
vacuum	46.4	43.2	20.2	18.6
CH <sub>2</sub> Cl <sub>2</sub>	47.9	41.0	15.2	2.8

chloromethane (DCM) being the commonly used solvent for alkane hydroxylation, we estimated its influence by single-point COSMO<sup>31</sup> calculations utilizing the optimized gas-phase geometries. These indicate hardly a DCM solvation effect on the O–O bond homolysis, but the activation and especially the reaction energy for the concerted reaction decrease by a significant 5.0 and 15.8 kcal mol<sup>-1</sup> (Table 1). The calculations then suggest that the peroxy O–O bond of *m*-CPBA does not cleave homolytically at room temperature, but that the presence of an alkane is needed. This, in fact, concurs with the experimental observation that at room temperature small amounts of radical derived side products are formed only in the presence of the alkane.<sup>8</sup> Larger amounts of such products result at higher temperatures<sup>8,24</sup> because either the free radical pathway(s) become accessible or diffusion of the intermediate radicals in the [2–H<sub>2</sub>O–6] triad competes with the concerted reaction.

The non-free-radical synchronous mechanism is consistent with the experimentally observed stereoselectivity. After formation of the meta-stable butyl radical, water, and *m*-chlorobenzoate radical triad [2–H<sub>2</sub>O–6], C–O bond formation to the alcohol proceeds barrier-free, indicating that the stereochemistry of the carbon center is maintained during this process. Disrupting the triad by removing the water molecule is slightly exothermic (2.6 kcal mol<sup>-1</sup>) and gives the butyl and *m*-chlorobenzoate radical pair. This unwanted side process provides a rationale for the presence of minor amounts of free radical derived side products.

In summary, the hydrocarbon hydroxylation by *m*-CPBA appears to be a nonconcerted synchronous mechanism.

**Comparison with P450 Chemistry.** There are analogies between the stereo- and regioselective hydroxylation of alkanes by peroxyacids and that by cytochromes P450. Both have been explained by concerted and (free) radical oxygen insertions. In the present discussion on the peroxy acid hydroxylation, both the peroxy acid and its alkanolate radical are considered as oxidants reacting in respectively a concerted or stepwise manner. Likewise, the iron porphyrin hydroperoxo species, Compound 0 (Cmpd 0), has been considered as a possible oxidant in the recent literature<sup>34–36</sup> in addition to the iron(IV) oxo porphyrin  $\pi$ -cation radical, Compound I (Cmpd I), that is commonly believed to be the reactive intermediate in cytochromes P450. It is presumed that Cmpd 0 reacts in a concerted fashion, whereas Cmpd I reacts in a stepwise manner via discrete radicals. This duality in pathways for the noncatalytic, nonenzymatic peroxyacid and the catalytic, enzymatic cytochrome P450 oxidations, together with the similarities of the hydroperoxo species for both, encouraged us to address the hydroxylation by cytochromes' P450 of particularly Cmpd 0 in analogy to that for the peroxyacid oxidation.

The P450 Cmpd 0 intermediate and the *m*-CPBA molecule show structural similarities (Figure 2). The O–O distances for Cmpd 0 and *m*-CPBA of respectively 1.422 and 1.423 Å are the same. Likewise, the angles between the O–H and O–O bonds and between the O–O and O–Fe/C bonds are comparable.

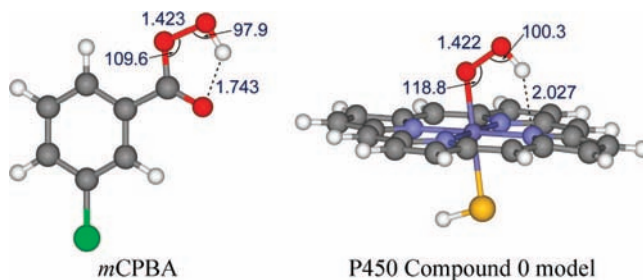


**Figure 2.** Optimized geometries for *m*-CPBA and the hydroperoxo iron porphyrin and selected bond distances (Å) and bond angles (deg).

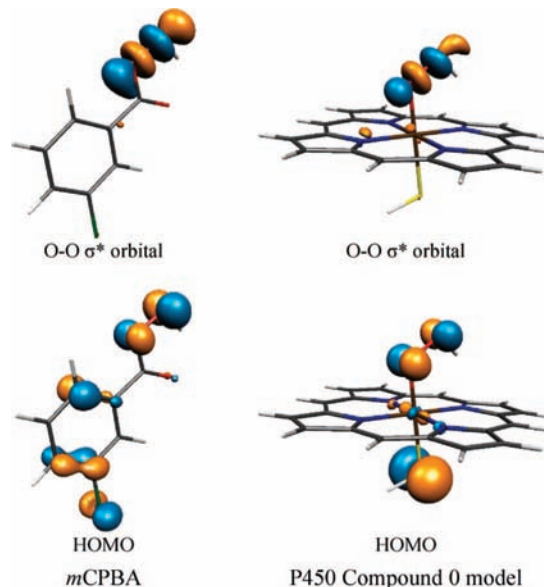


**Figure 3.** HOMO's and selected unoccupied MO's of *m*-CPBA and Compound 0.

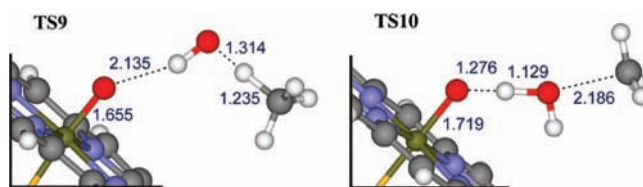


**Figure 4.** Transition structures TS9 and TS10 of Scheme 9 with selected bond distances (Å).

Orbital analysis shows similar HOMO's for Cmpd 0 and *m*-CPBA of a  $\pi^*$ -oxygen nonbonding nature (Figure 3). Homolytic O–O bond cleavage involves electron transfer from this HOMO to the O–O antibonding  $\sigma^*$  orbital for which the energy difference is 0.5 eV less for Cmpd 0 than for *m*-CPBA. This is reflected in the energetics of the alkane assisted reaction. The O–O bond homolysis for Cmpd 0 has a smaller barrier (16.6 kcal mol<sup>-1</sup>) than that for *m*-CPBA (20.2 and 23.8 kcal mol<sup>-1</sup>, for butane and propane, respectively).

Cmpd 0 hydroxylation starts by homolytic cleavage of the O–O bond (Scheme 8, **18**  $\rightarrow$  **TS8**  $\rightarrow$  **22**). H-atom abstraction from the alkane, calculated for both methane and propane, by the generated hydroxyl radical via transition state **TS9** (Figure 4) gives the intermediate iron–oxo–water–alkyl radical triad **23a**, which is isoenergetic with the reactants (**18**). The H-atom of the newly formed water molecule in triad **23a** is pointing toward the methyl radical. Only a small reorientation of both units in such a manner that the oxygen points toward the carbon radical suffices to give the virtually isoenergetic triad **23b**. Subsequent homogenic C–O bond formation between the alkyl

radical and the water molecule with a simultaneous H-shift from water to the iron-oxo moiety (TS10, Figure 4) results in the exothermic formation of the alcohol (methanol or propanol) and the resting state (Scheme 8). This mechanism represents a two step process and differs from the nonconcerted synchronous mechanism for the hydroxylation by *m*-CPBA. The first difference is the presence of a metastable minimum after the homolytic O–O bond cleavage due to the stabilization of the iron-oxo species (Cmpd II). However, the subsequent barrier for H-abstraction is very small so that once the O–O bond is cleaved to form the reactive hydroxyl radical **22** the reaction continues to give the Cmpd II-water-alkyl radical triad **23**. The relative high stability of this triad (**23**) compared to that (2–H<sub>2</sub>O–**6**) for the *m*-CPBA induced reaction constitutes the major difference in reaction mechanisms. Due to the relative stability of triad **23**, the barrier for subsequent homogenic C–O bond formation to give the alcohol is relatively high and makes this pathway a two-step mechanism instead of a concerted one.

In summary, the hydrocarbon hydroxylation by peroxy acids is best described by a synchronous nonconcerted mechanism. A comparable mechanism for the alkane hydroxylation by porphyrin P450 Cmpd 0, would represent a two-step process. Of course, this analysis focuses only on Cmpd 0 of a model system. It does not address the enzyme environment<sup>37</sup> or proton delivery channels. Neither does it attempt to provide balance against alternative pathways such as the porphyrin attack by the incipient OH radical,<sup>38</sup> those by Cmpd I, or the shunt mechanism. However, the presented comparison addresses an aspect that received modest attention in the decades old search in unraveling the mechanism of the cytochromes P450 catalytic cycle.

## Conclusion

This study provides the first comprehensive analysis of the reaction mechanism of the alkane hydroxylation by *m*-chloroperoxybenzoic acid using density functional theory. The calculations indicate the oxidation to be a nonconcerted synchronous peroxy oxygen insertion into the C–H bond of the alkane. This pathway is energetically favored over alternative stepwise radical processes.

Alkane hydroxylation by the hydroperoxy Compound 0 intermediate of cytochromes P450 shows resemblance to that by *m*-CPBA. However, due to the intrinsic stability of the Cmpd II intermediate that is involved in the process, the P450–Cmpd 0 governed reaction represents a nonsynchronous two-step reaction. In the *m*-PCBA hydroxylation this intermediate is not stabilized and converts barrier-free to the alcohol product.

**Acknowledgment.** The Center of Complex Molecules of the VU University, Amsterdam, is acknowledged for financial support and the National Computing Facilities Foundation (NCF) for the use of their supercomputer facilities with financial support from The Netherlands Organization for Scientific Research (NWO).

**Supporting Information Available:** Cartesian coordinates, energies and salvation energies of the optimized structures (7 pages). This material is available free of charge via the Internet at <http://pubs.acs.org>.

## References and Notes

- (1) *The Chemistry of Functional Groups. Peroxides*; Patai, S., Ed.; John Wiley: New York, 1983.
- (2) Hassall, C. H. *Org. React.* **1957**, *9*, 73–106.
- (3) Sawaki, Y. *Organic Peroxides*; Ando, W. Ed.; John Wiley: Chichester, U.K., 1992; pp 425–477.
- (4) Deno, N. C.; Jedziniak, E. J.; Messer, L. A.; Meyer, M. D.; Stroud, S. G.; Tomezko, E. S. *Tetrahedron* **1977**, *33*, 2503.
- (5) Frommer, U.; Ullrich, V. *Z. Naturforsch. B* **1971**, *26*, 322–327.
- (6) Schneider, H.-J.; Müller, W. *J. Org. Chem.* **1985**, *50*, 4609–4615.
- (7) Smith, J. R. L.; Sleath, P. R. *J. Chem. Soc., Perkin Trans. 2* **1983**, 1165–1169.
- (8) Bravo, A.; Bjorsvik, H.-R.; Fontana, F.; Minisci, F.; Serri, A. *J. Org. Chem.* **1996**, *61*, 9409–9416.
- (9) In the oxidation of adamantane by *m*-CPBA, chlorobenzene is formed in CH<sub>2</sub>Cl<sub>2</sub>, CHCl<sub>3</sub> solution S and *m*-chlorobiphenyl is formed in benzene solution, which involves decarboxylation of *m*-chlorobenzoyloxy radical (eq 7).
- (10) Fossey, J.; Lefort, D.; Sorba, J. In *Free Radicals in Organic Chemistry*; Wiley: New York, 1995.
- (11) In the oxidation of cyclohexane-*d*<sub>12</sub> by TFPA, CO<sub>2</sub> and fluoroform-*d* is formed as side products.
- (12) Camaioni, D. M.; Bays, J. T.; Shaw, W. J.; Linehan, J. C.; Birnbaum, J. C. *J. Org. Chem.* **2001**, *66*, 789–795.
- (13) Freccero, M.; Gandolfi, R.; Sarzi-Amade, M.; Rastelli, A. *Tetrahedron* **2001**, *57*, 9843–9848.
- (14) Mimoun, H. *Angew. Chem., Int. Ed. Engl.* **1982**, *21*, 734.
- (15) Porter, N. A.; Yin, H.; Pratt, D. A. *J. Am. Chem. Soc.* **2000**, *122*, 11272–11273.
- (16) (a) Ortiz de Montellano, P. R., Ed. *Cytochrome P450: Structure, Mechanism and Biochemistry*, 3rd ed.; Kluwer Academic/Plenum Publishers: New York, 2005. (b) Denisov, I. G.; Markis, T. M.; Sligar, S. G.; Schlichting, I. *Chem. Rev.* **2005**, *105*, 2253. (c) Sono, M.; Roach, M. P.; Coulter, E. D.; Dawson, J. H. *Chem. Rev.* **1996**, *96*, 2841.
- (17) (a) Groves, J. T.; McClusky, G. A. *J. Am. Chem. Soc.* **1976**, *98*, 859. (b) Groves, T.; McClusky, G. A.; White, R. E.; Coon, M. J. *Biochem. Biophys. Res. Commun.* **1978**, *81*, 154.
- (18) (a) Schöneboom, J. C.; Cohen, S.; Lin, H.; Shaik, S.; Thiel, W. *J. Am. Chem. Soc.* **2004**, *126*, 4017. (b) Schöneboom, J. C.; Lin, H.; Reuter, N.; Thiel, W.; Cohen, S.; Ogliaro, F.; Shaik, S. *J. Am. Chem. Soc.* **2002**, *124*, 8142. (c) Ogliaro, F.; De Visser, S. P.; Cohen, S.; Kaneti, J.; Shaik, S. *ChemBiochem* **2001**, *11*, 848. (d) Ogliaro, F.; Harris, N.; Cohen, S.; Filatov, M.; De Visser, S. P.; Shaik, S. *J. Am. Chem. Soc.* **2000**, *122*, 8977.
- (19) Mueller, E. J. P. J. Loida, S. G. *Sligar in Cytochrome P450: Structure, Mechanism and Biochemistry* 2nd ed.; Ortiz de Montellano, P. R. Plenum Press: New York, 1995; pp 83–124.
- (20) (a) Shaik, S.; Kumar, D.; De Visser, S. P.; Altun, A.; Thiel, W. *Chem. Rev.* **2005**, *105*, 2279–2328. (b) Meunier, B.; De Visser, S. P.; Shaik, S. *Chem. Rev.* **2004**, *104*, 3947–3980. (c) Loew, G. H.; Harris, D. J. *Chem. Rev.* **2000**, *100*, 407–419. (d) Rydberg, P.; Sigfridsson, E.; Ryde, U. *J. Biol. Inorg. Chem.* **2004**, *9*, 203–223.
- (21) (a) Jin, S.; Bryson, T. A.; Dawson, J. H. *J. Biol. Inorg. Chem.* **2004**, *9*, 644. (b) Nam, W.; Ryu, Y. O.; Song, W. J. *J. Biol. Inorg. Chem.* **2004**, *9*, 654. (c) Shaik, S.; de Visser, S. P.; Kumar, D. *J. Biol. Inorg. Chem.* **2004**, *9*, 661–668. (d) Newcomb, M.; Hollenberg, P. F.; Coon, M. J. *Arch. Biochem. Biophys.* **2003**, *409*, 72.
- (22) (a) Newcomb, M.; Chandrasena, R. E. P. *Biochem. Biophys. Res. Commun.* **2005**, *338*, 394–403. (b) Newcomb, M.; Hollenberg, P. F.; Coon, M. J. *Arch. Biochem. Biophys.* **2003**, *409*, 72–79.
- (23) Kumar, D.; Hirao, H.; De Visser, S. P.; Zheng, J.; Wang, D.; Thiel, W.; Shaik, S. *J. Phys. Chem. B* **2005**, *109*, 19946.
- (24) (a) Derat, E.; Kumar, D.; Hirao, H.; Shaik, S. *J. Am. Chem. Soc.* **2006**, *128*, 473. (b) Bach, R. D.; Dmitrenko, O. *J. Am. Chem. Soc.* **2006**, *128*, 1474–1488.
- (25) (a) Ortiz de Montellano, P. R.; De Voss, J. J. *Nat. Prod. Rep.* **2002**, *19*, 477–493. (b) Chandrasena, R. E. P.; Vatsis, K. P.; Coon, M. J.; Hollenberg, P. F.; Newcomb, M. *J. Am. Chem. Soc.* **2004**, *126*, 115. (c) Newcomb, M.; Aebischer, D.; Shen, R.; Chandrasena, R. E. P.; Hollenberg, P. F.; Coon, M. J. *J. Am. Chem. Soc.* **2003**, *125*, 6064. (d) Newcomb, M.; Chandrasena, R. E. P. *Biochem. Biophys. Res. Commun.* **2005**, *338*, 394. (e) Raag, R.; Martinis, S. A.; Sligar, S. G.; Poulos, T. L. *Biochemistry* **1991**, *30*, 11420. (f) Newcomb, M.; Shen, R.; Choi, S. Y.; Toy, P. H.; Hollenberg, P. F.; Vaz, A. D. N.; Coon, M. J. *J. Am. Chem. Soc.* **2000**, *122*, 2677. (g) Davydov, R.; Perera, R.; Jin, S.; Yang, T.-C.; Bryson, T. A.; Sono, M.; Dawson, J. H.; Hoffman, B. M. *J. Am. Chem. Soc.* **2005**, *127*, 1403. (h) Coon, M. J. *Biochem. Biophys. Res. Commun.* **2003**, *312*, 163.
- (26) (a) White, R. E.; Coon, M. J. *Annu. Rev. Biochem.* **1980**, *49*, 315–356. (b) Correia, M. A.; Yao, K.; Allentoff, A. J.; Wrighton, S. A.; Thompson, J. A. *Arch. Biochem. Biophys.* **1995**, *317*, 471–478. (c) Thompson, J. A.; Yumibe, N. P. *Drug Metab. Rev.* **1989**, *20*, 365–378. (d) Lee, W. A.; Bruice, T. C. *J. Am. Chem. Soc.* **1985**, *107*, 513–514. (e) Barr, D. P.; Martin, M. V.; Guengerich, F. P.; Mason, R. P. *Chem. Res. Toxicol.* **1996**, *9*, 318–325. (f) White, R. E.; Sligar, S. G.; Coon, M. J. *J. Biol. Chem.* **1980**, *255*, 11108–11111. (g) Blake, R. C.; Coon, M. J. *J. Biol. Chem.* **1981**, *256*, 12127–12133. (h) Schunemann, V.; Lendzian, F.; Jung, C.; Contzen, J.; Barra, A.-L.; Sligar, S. G.; Trautwein, A. X. *J. Biol. Chem.* **2004**, *279*, 10919–10930. (i) Schunemann, V.; Jung, C.; Terner, J.; Trautwein, A. X.;

Weiss, R. *J. Inorg. Biochem.* **2002**, *91*, 586–596. (j) Schunemann, V.; Jung, C.; Trautwein, A. X.; Mandon, D.; Weiss, R. *FEBS Lett.* **2000**, *479*, 149–154.

(27) (a) Bach, R. D.; Dmitrenko, O. *J. Am. Chem. Soc.* **2006**, *128*, 1474–1488. (b) Derat, E.; Kumar, D.; Hirao, H.; Shaik, S. *J. Am. Chem. Soc.* **2006**, *128*, 473–484. (c) Groenhof, A. R.; Ehlers, A. W.; Lammertsma, K. Submitted for publication.

(28) (a) Te Velde, G.; Bickelhaupt, F. M.; Van Gisbergen, S. J. A.; Fonseca Guerra, C.; Baerends, E. J.; Snijders, J. G.; Ziegler, T. *J. Comput. Chem.* **2001**, *22*, 931. (b) Fonseca Guerra, C.; Snijders, J. G.; Te Velde, G.; Baerends, E. J. *Theor. Chem. Acc.* **1988**, *99*, 391. *ADF2005.01*; SCM, Theoretical Chemistry, Vrije Universiteit, Amsterdam, The Netherlands, <http://www.scm.com>.

(29) Handy, N. C.; Cohen, A. J. *Mol. Phys.* **2001**, *99*, 403.

(30) Perdew, J. P.; Burke, K.; Ernzerhof, M. *Phys. Rev. Lett.* **1996**, *77*, 3865.

(31) (a) Pye, C. C.; Ziegler, T. *Theor. Chem. Acc.* **1999**, *101*, 396–408. (b) Klamt, A.; Schuurmann, G. *J. Chem. Soc., Perkin Trans. 2* **1993**, 799–805. (c) Klamt, A. *J. Phys. Chem.* **1995**, *99*, 2224–2235. (d) Klamt, A.; Jones, V. *J. Chem. Phys.* **1996**, *105*, 9972–9981.

(32) Recent experimental determinations in the gas phase gave an average value of 42.9 kcal/mol for the O–O bond strength; c.f.: Borges dos Santos, R. M.; Muralha, V. S. F.; Correia, C. F.; Martinho Simões, J. A. *J. Am. Chem. Soc.* **2001**, *123*, 12670–12674.

(33) Either decreasing the O194 > H distance or increasing the C–H distance in geometry scans results in exothermic and barrierless processes.

(34) (a) Groves, J. T.; McClusky, G. A. *J. Am. Chem. Soc.* **1976**, *98*, 859–861. (b) Groves, J. T.; McClusky, G. A.; White, R. E.; Coon, M. *J. Biochem. Biophys. Res. Commun.* **1978**, *81*, 154–160.

(35) Ortiz de Montellano, P. R. *Cytochrome P450: Structure, Mechanism and Biochemistry*, 3rd ed.; Kluwer Academic/Plenum Publishers: New York, 2005.

(36) Newcomb, M.; Chandrasena, R. E. P. *Biochem. Biophys. Res. Commun.* **2005**, *338*, 394–403.

(37) Zheng, J.; Wang, D.; Thiel, W.; Shaik, S. *J. Am. Chem. Soc.* **2006**, *128*, 13204–13215.

(38) Sharma, P. K.; Kevorkiants, R.; de Visser, S. P.; Kumar, D.; Shaik, S. *Angew. Chem., Int. Ed.* **2004**, *43*, 1129–1132.

JP801720S